[redacted]

NASA TECHNICAL MEMORANDUM

NASA TM X-73948

COPY NO.

NASA TM X-73948

DEVELOPMENT OF TWO SUPERCRITICAL AIRFOILS WITH A THICKNESS-TO-CHORD RATIO OF 0.20 AND DESIGN LIFT COEFFICIENTS OF 0.3 AND 0.4

by Lloyd S. Jernell

September 1, 1976

NASA
National Aeronautics and Space Administration

Langley Research Center
Hampton, Virginia 23665

[redacted]

[redacted]

1. Report No.	2. Government Accession No.	3. Recipient's Catalog No.
TM X-73948		

4. Title and Subtitle	5. Report Date
DEVELOPMENT OF TWO SUPERCRITICAL AIRFOILS WITH A THICKNESS-TO-CHORD RATIO OF 0.20 AND DESIGN LIFT COEFFICIENTS OF 0.3 AND 0.4	September 1, 1976
	6. Performing Organization Code: 31.600

7. Author(s)	8. Performing Organization Report No.
Lloyd S. Jernell	
	10. Work Unit No.
9. Performing Organization Name and Address: NASA Langley Research Center, Hampton, VA 23665	11. Contract or Grant No.
	13. Type of Report and Period Covered: Technical Memorandum
12. Sponsoring Agency Name and Address: National Aeronautics & Space Administration, Washington, DC 20546	14. Sponsoring Agency Code

15. Supplementary Notes

16. Abstract

Two supercritical airfoils have been developed specifically for application to span distributed loading cargo aircraft. These airfoils have a thickness-to-chord ratio of 0.20 and design lift coefficients of 0.3 and 0.4, and have been derived by modifying a recently developed supercritical airfoil having a thickness-to-chord ratio of 0.18 and a design lift coefficient of 0.5. The aerodynamic characteristics were calculated using a theoretical method which computes the flow field about an airfoil having supercritical surface velocities.

17. Key Words (Suggested by Author(s))

Supercritical Airfoils
Transonic Aerodynamics
Spanloaded Cargo Aircraft

19. Security Classif. (of this report)	20. Security Classif. (of this page)	21. No. of Pages
[redacted]	Unclassified	26

DEVELOPMENT OF TWO SUPERCRITICAL AIRFOILS WITH A THICKNESS-TO-CHORD RATIO OF 0.20 AND DESIGN LIFT COEFFICIENTS OF 0.3 AND 0.4

by Lloyd S. Jernell
NASA Langley Research Center

SUMMARY

Two supercritical airfoils have been developed specifically for application to span-distributed loading cargo aircraft. These airfoils have a thickness-to-chord ratio of 0.20 and design lift coefficients of 0.3 and 0.4 (designated airfoils 3-20 and 4-20, respectively), and have been derived by modifying a recently developed supercritical airfoil having a thickness-to-chord ratio of 0.18 and a design lift coefficient of 0.5. The aerodynamic characteristics were calculated using the Bauer-Garabedian-Korn theoretical method which computes the flow field about an airfoil having supercritical surface velocities.

Theory predicts shockless flow about both airfoils at $M = 0.69$.

At subcritical Mach numbers, the calculated pressure distribution over portions of the airfoil differs somewhat from that predicted by the modified Lockheed subsonic airfoil program.

At design lift coefficient, theory predicts the same magnitude of drag for both airfoils prior to the supercritical drag rise, which begins at $M = 0.70$ for airfoil 3-20 and $M = 0.69$ for airfoil 4-20. The drag values are in close agreement with those of the modified Lockheed method at subcritical Mach numbers.

The effect of Mach number on pitching-moment coefficient is small. Both airfoils exhibit appreciable negative moments about the quarter chord, with that of the 4-20 airfoil being greater. The modified Lockheed method predicts a considerably greater negative moment in the subcritical Mach number range.

At $M = 0.69$ no large areas of boundary-layer separation are predicted for airfoil 3-20 except at lift coefficients corresponding to maneuver loads lesser than approximately -1g and greater than approximately 3g. However, for airfoil 4-20 extensive separation exists for maneuver loads below about 0.5g and above about 2g.

INTRODUCTION

Both NASA and the aircraft industry are currently studying the problems associated with the design and operation of very large long-range subsonic transport aircraft, with emphases on the utilization of cargo containers and a payload capability much greater than those of current aircraft. A design

concept which holds promise for application to such an airplane is that of distributing the payload along the wing span to counterbalance the aerodynamic loads, with a resultant decrease in wing bending moments and shear forces, and thus decreased structural weight. Studies of the technical and economic aspects of distributed load aircraft, wherein cargo containers of 8' x 8' cross section are carried within the wing, are documented in references 1 to 3. These studies indicate that an airplane of this type would require an airfoil with a thickness-to-chord ratio of about 0.20 and a section lift coefficient in the range of 0.3 to 0.4.

Since this aircraft would require an unusually thick wing, the use of a supercritical airfoil of the type discussed in reference 4 is essential in order to attain a reasonably high cruise speed. Although considerable research has been conducted recently in the development of this type airfoil, much of the data are as yet unpublished (the experimental results for 10- and 14-percent thick airfoils are reported in references 5 and 6, respectively). Also, the work performed to date has been limited to airfoils of lower thickness-to-chord ratios and higher design section lift coefficients than required for distributed load aircraft.

The purpose of this study was to develop two supercritical airfoils which would be applicable to spanloader aircraft. These airfoils have a thickness-to-chord ratio of 0.20 and design section lift coefficients of 0.30 and 0.40.

SYMBOLS

c	airfoil chord
c_d	drag coefficient, $\frac{\text{Drag}}{qc}$
$c_{d,\text{wave}}$	wave drag coefficient
c_l	lift coefficient, $\frac{\text{Lift}}{qc}$
c_m	pitching-moment coefficient about quarter chord, $\frac{\text{Pitching Moment}}{qc^2}$
C_p	pressure coefficient
g	gravitational constant
M	free-stream Mach number
q	free-stream dynamic pressure
t	airfoil maximum thickness

x	airfoil longitudinal coordinate
x_{sep}	beginning of separated-flow region, measured from airfoil leading edge
y	airfoil vertical coordinate
α	angle of attack, deg.

COMPUTER PROGRAM

The data were computed using the supercritical airfoil analysis program described in references 7 and 8. However, the program version employed has been modified to reduce computer time and to yield slightly lower wave drag. The method uses finite difference equations to obtain steady transonic solutions to the equations of motion of an inviscid, compressible fluid about a profile which includes the airfoil and its boundary layer. The program employs the semi-empirical methods of reference 9 to compute the boundary layer thickness and separation location. Although the method has been modified to account for increased thickness in the region of separated flow, the validity of these modifications remain to be proven, especially at the high Reynolds numbers considered herein where no experimental data exists for comparison.

DISCUSSION

Prior to this project, one method which was briefly considered for developing a supercritical airfoil applicable to distributed load aircraft was that of simply scaling the vertical coordinates of an available supercritical airfoil of lesser thickness to provide a $t/c = 0.20$. An airfoil similar to that investigated in reference 6, having a $t/c = 0.14$ and a design of C_l of approximately 0.7, was modified in this manner. The resultant airfoil, its pressure distribution, and supersonic flow areas are shown in figure 1 as calculated by the analysis program. The airfoil profile also includes the boundary layer. For all cases presented herein viscous effects were calculated for a Reynolds number of 100×10^6 and transition to turbulent flow at the 8 percent chord location.

The greatest fallacy in this approach is that by increasing the airfoil vertical coordinates, the effective camber also is increased by a comparable magnitude, resulting in the airfoil in figure 1 having a design lift coefficient of about 1.0. Operating this airfoil at a C_l needed for distributed load aircraft (in this case $C_l = 0.40$) requires a negative angle of attack and, as indicated by the pressure distribution, results in negative lift over approximately the forward 23 percent of the airfoil. In addition, the location of the center of pressure at roughly the three-quarter chord station produces an unreasonably high negative pitching moment. The analysis program indicates that separation shall occur on the upper and lower surfaces at the 94- and 68-percent chord

stations, respectively. As previously mentioned, the data are unreliable when extensive separation exists; however, the results are believed to be accurate enough to exemplify some of the shortcomings of this type of modification.

The approach employed in the development of the two airfoils of the present study was that of altering independently the thickness and camber of an existing supercritical airfoil which appeared to most nearly satisfy the overall distributed load aircraft requirements. This technique allows the designer to trade lift coefficient for thickness. The airfoil chosen for modification had a $t/c = 0.18$ and a design $C_l = 0.5$, and was developed by Charles D. Harris of the Langley Research Center using the method employed in the design of the airfoils of references 5 and 6.

For the above airfoil, data from the analysis program indicated that at the design C_l and M (approximately 0.71), the angle of attack was nearly zero. Since at zero angle-of-attack the lift of an airfoil is approximately a linear function of the amount of camber, the magnitude of the original mean line was reduced by factors of 0.6 and 0.8 to provide section lift coefficients of 0.3 and 0.4, respectively. Also, the thickness was increased to $t/c = 0.20$. These coordinates were then used in the analysis program to determine the characteristics of the new airfoils at Mach numbers just below the drag-divergence region. At the highest shockless Mach number, which was approximately 0.69 for each airfoil, it was found that the pressure distribution was generally of the shape desired. However, adjustments were made in the pressure profile by minor refairing along selected segments of the airfoil surface. The resultant profiles are designated airfoils 3-20 and 4-20. The first digit indicates the design lift coefficient in tenths. The digits following the hyphen denote the airfoil thickness in percent of chord. The airfoil coordinates are tabulated in tables I and II.

The profile for airfoil 3-20 (including the boundary layer), its supersonic flow region, and pressure distribution are shown in figure 2 for the design lift coefficient and Mach numbers from 0.69 to 0.72. At $M = 0.69$ (fig. 2(a)) theory predicts shockless supersonic flow over most of the forward section of the upper surface. The pressure distribution is relatively constant in the supersonic flow region and exhibits a favorable gradient over approximately the forward half of the lower surface. For the rearward sections of both the upper and lower surfaces the data indicate a relatively mild pressure recovery. As Mach number is increased to 0.72, the pressure gradient over the forward upper surface becomes increasingly favorable, followed by the development of a weak recompression near the midchord. There is little Mach number effect on the C_p distribution over the rearward upper surface. Although the C_p distribution over the lower surface varies little as Mach number is increased, the data indicate the rapid development of a supersonic flow region over the forward section.

Data for the 4-20 airfoil are presented in figure 3 for Mach numbers from 0.69 to 0.71. In general, the comments regarding figure 2 also apply to these data since the shapes of the pressure distributions and supersonic flow regions for both airfoils basically are quite similar.

Comparisons of the pressure distributions as predicted by the analysis program and by an improved version of the computer program described in reference 10 (which is a modification of the Lockheed program presented in reference 11) for the 4-20 airfoil at the design lift coefficient are shown in figure 4. It should be recognized that the two treatments of the airfoil problem differ significantly in a number of ways. First, the analysis program operates with a finite-difference scheme utilizing basic equations valid for subsonic, transonic, and supersonic flow. The modified Lockheed method represents the airfoil piecewise as a distribution of vortex sheets and performs an incompressible calculation of the velocities and pressures. These values are then adjusted for compressibility by utilizing the Karman-Tsien relationship. This latter scheme obviously is inadequate where the local flow is supersonic, as in figure 4(a).

Secondly, the modified Lockheed method calculates both the laminar and turbulent boundary layer when adjusting the airfoil coordinates to account for boundary layer displacement thickness, with elaborate schemes to identify transition if desired; or, alternately, transition location may be specified. The analysis method ignores the laminar boundary layer and starts a fresh turbulent boundary layer at the specified transition point. Obviously there will be some difference in the resultant effective airfoil shapes.

Thirdly, the modified Lockheed method fixes the trailing-edge condition by placing constraints on the first and last vorticity elements so as to require equal pressures above and below the trailing edge. The numerical treatment actually results in moving this equal-pressure point slightly forward of the trailing edge. The analysis method places constraints on the dividing streamline that essentially requires a zero pressure gradient across the entire wake; however, the turbulent boundary layer at the trailing edge is modified so as to force a pressure distribution near the trailing edge that is similar to that observed in the wind tunnel (see ref. 8).

It is beyond the scope of this paper to examine the validity of all these items; however, figure 4 shows that the pressure distributions obtained by the two methods are somewhat different. In particular, as will be shown subsequently, the differences in the pressure distribution over the rearward portion of the airfoil lead to significant differences in pitching moment.

The effects of Mach number on wave drag at the design lift coefficient as computed by the analysis program are shown in figure 5. For both airfoils wave drag begins developing at $M = 0.70$ and, as expected, increases with Mach number at a higher rate for the 4-20 airfoil due to its greater camber.

Figure 6 shows the Mach number effects on total drag coefficient at the design lift coefficient for both airfoils using the analysis program and the method of reference 10 as well for airfoil 4-20. The methods are in close agreement in the Mach number range preceding the major drag rise, with each indicating a slight increase in drag coefficient with increasing Mach number. The analysis program exhibits the same magnitude of drag for both airfoils prior to the drag rise. As previously mentioned, for both airfoils the wave drag begins developing at $M = 0.70$. This is the approximate Mach number at which

the total drag rise begins for airfoil 3-20. However, the total drag rise for airfoil 4-20 begins at $M = 0.69$ due to a predicted increase in profile drag beginning at this Mach number.

The effects of Mach number on pitching-moment coefficient as predicted by the analysis program and the method of reference 10 are shown in figure 7. For all cases presented the Mach number effects are minor. The analysis program data indicate that the 4-20 airfoil has slightly greater negative pitching-moment than the 3-20 airfoil. For the 4-20 airfoil, the method of reference 10 predicts a greater negative pitching-moment, due to the greater rearward loading of the airfoil as exhibited by the pressure distributions of figure 4.

Figure 8 shows the effects of lift coefficient on boundary layer separation for the two airfoils at $M = 0.69$ as predicted by the analysis program. As previously mentioned, the validity of the method used in computing boundary layer thickness in regions of separated flow is questionable. Hence, for the cases considered in this report wherein extensive areas of separation are predicted, the data should be used with caution. As indicated in figure 8, no large areas of separation are predicted for airfoil 3-20 except at lift coefficients approximating maneuver loads of -1g and 3g. However, for airfoil 4-20 extensive separation exists over the lower surface at lift coefficients below about 0.2 and over the upper surface at lift coefficients greater than that corresponding to a 2g maneuver load.

The aerodynamic characteristics for airfoil 3-20 at $M = 0.69$ are presented in figure 9. The pitching-moment exhibits slightly positive stability about the quarter-chord position. The lift-curve slope is approximately linear for the lift coefficients considered. The drag coefficient varies little at lift coefficients below approximately 0.6.

The aerodynamic characteristics for airfoil 4-20 at $M = 0.69$, shown in figure 10, exhibit trends similar to those of airfoil 3-20. However, the data for lift coefficients below approximately 0.2 and above about 0.8 should be used with caution due to the relatively large areas of predicted flow separation as shown in figure 8.

CONCLUSIONS

Two supercritical airfoils have been developed specifically for application to span-distributed loading cargo aircraft. These airfoils have a thickness-to-chord ratio of 0.20 and design lift coefficients of 0.3 and 0.4, and have been derived by modifying a recently-developed supercritical airfoil having a thickness-to-chord ratio of 0.18 and a design lift coefficient of 0.5. The aerodynamic characteristics were calculated using a theoretical method which computes the flow field about an airfoil having supercritical surface velocities. The conclusions are as follows:

1. Theory predicts shockless flow about both airfoils at $M = 0.69$.

2. At subcritical Mach numbers, the calculated pressure distribution over portions of the airfoil differs somewhat from that predicted by the modified Lockheed subsonic airfoil program.

3. At design lift coefficient, theory predicts the same magnitude of drag for both airfoils prior to the supercritical drag rise, which begins at $M = 0.70$ for airfoil 3-20 and $M = 0.69$ for airfoil 4-20. The drag values are in close agreement with those of the modified Lockheed method at subcritical Mach numbers.

4. The effect of Mach number on pitching-moment coefficient is small. Both airfoils exhibit appreciable negative moments about the quarter chord, with that of the 4-20 airfoil being greater. The modified Lockheed method predicts a considerably greater negative moment in the subcritical Mach number range.

5. At $M = 0.69$, no large areas of boundary-layer separation are predicted for airfoil 3-20 except at lift coefficients corresponding to maneuver loads lesser than approximately -1g and greater than approximately 3g. However, for airfoil 4-20 extensive separation exists for maneuver loads below about 0.5g and above about 2g.

REFERENCES

1. Whitener, C. P.; Gratzer, B. L.; and Whitlow, D. H.: Technical and Economic Assessment of Span-Distributed Loading Cargo Aircraft Concepts. Boeing Company, NASA CR-144963, 1976.

2. Malthan, V. L.: Technical and Economic Assessment of Span-Distributed Loading Cargo Aircraft Concepts. Douglas Aircraft Company, NASA CR-144962, 1976.

3. Johnston, W. M.; Muehlbauer, J. C.; Eudaily, R. R.; Farmer, B. T.; Honrath, J. F.; and Thompson, S. G.: Technical and Economic Assessment of Span-Distributed Loading Cargo Aircraft Concepts. Lockheed-Georgia Company, NASA CR-145034, 1976.

4. Whitcomb, Richard T.: Review of NASA Supercritical Airfoils. ICAS Paper No. 74-10, 1974.

5. Harris, Charles D.: Aerodynamic Characteristics of the 10-Percent-Thick NASA Supercritical Airfoil 33 Designed For a Normal-Force Coefficient of 0.7. NASA TM X-72711, 1975.

6. Harris, Charles D.: Aerodynamic Characteristics of a 14-Percent-Thick NASA Supercritical Airfoil Designed for a Normal-Force Coefficient of 0.7. NASA TM X-72712, 1975.

7. Bauer, F.; Garabedian, P.; and Korn, D.: Supercritical Wing Sections. Lecture Notes in Economics and Mathematical Systems, M. Beckmann and H. P. Kunzi, eds., Springer-Verlag, 1972.

8. Bauer, F.; Garabedian, P.; Korn, D.; and Jameson, A.: Supercritical Wing Sections II. Lecture Notes in Economics and Mathematical Systems, M. Beckmann and H. P. Kunzi, eds., Springer-Verlag, 1975.

9. Nash, J. F.; and MacDonald, A. G. J.: The Calculation of Momentum Thickness in a Turbulent Boundary Layer at Mach numbers up to Unity. Aeronautical Research Council C. P. No. 963, 1967.

10. Smetana, Frederick O.; Summery, Delbert C.; Smith, Neill S.; and Carden, Ronald K.: Light Aircraft Lift, Drag, and Moment Prediction - A Review and Analysis. North Carolina State University, NASA CR-2523, 1975.

11. Stevens, W. A.; Goradia, S. H.; and Braden, J. A.: Mathematical Model for Two-Dimensional Multi-Component Airfoils in Viscous Flow. Lockheed-Georgia Company, NASA CR-1843, 1971.

[redacted]

TABLE I.- AIRFOIL 3-20 SECTION COORDINATES

$\frac{x}{c}$	$\frac{y}{c}$	
	UPPER SURFACE	LOWER SURFACE
0.00000	0.00000	0.00000
.00500	.02367	-.02367
.01000	.03234	-.03233
.02000	.04324	-.04322
.04000	.05650	-.05650
.06000	.06505	-.06501
.08000	.07136	-.07137
.10000	.07645	-.07642
.12000	.08065	-.08062
.14000	.08420	-.08420
.16000	.08723	-.08728
.18000	.08984	-.08995
.20000	.09208	-.09224
.22000	.09399	-.09420
.24000	.09561	-.09583
.26000	.09698	-.09719
.28000	.09806	-.09825
.30000	.09892	-.09906
.32000	.09955	-.09961
.34000	.09994	-.09987
.36000	.10009	-.09984

$\frac{x}{c}$	$\frac{y}{c}$	
	UPPER SURFACE	LOWER SURFACE
.38000	.10009	-.09955
.40000	.09985	-.09900
.42000	.09935	-.09812
.44000	.09859	-.09687
.46000	.09760	-.09534
.48000	.09633	-.09342
.50000	.09476	-.09102
.52000	.09283	-.08819
.54000	.09061	-.08498
.56000	.08814	-.08142
.58000	.08534	-.07754
.60000	.08230	-.07336
.62000	.07904	-.06896
.64000	.07567	-.06445
.66000	.07209	-.05979
.68000	.06833	-.05501
.70000	.06436	-.05008
.72000	.06031	-.04513
.74000	.05609	-.04013
.76000	.05178	-.03510
.78000	.04736	-.03020

[redacted]

(Cont'd)

TABLE I.- AIRFOIL 3-20 SECTION COORDINATES

$\frac{x}{c}$	$\frac{y}{c}$	
	UPPER SURFACE	LOWER SURFACE
.80000	.04287	-.02535
.82000	.03835	-.02065
.84000	.03376	-.01624
.86000	.02919	-.01215
.88000	.02471	-.00863
.90000	.02037	-.00585
.92000	.01621	-.00391
.94000	.01218	-.00294
.96000	.00822	-.00300
.98000	.00445	-.00421
1.00000	.00092	-.00674

TABLE II.- AIRFOIL 4-20 SECTION COORDINATES

$\frac{x}{c}$	$\frac{y}{c}$	
	UPPER SURFACE	LOWER SURFACE
0.00000	0.00000	0.00000
.00500	.02367	-.02367
.01000	.03234	-.03233
.02000	.04324	-.04322
.04000	.05650	-.05650
.06000	.06506	-.06500
.08000	.07136	-.07137
.10000	.07645	-.07642
.12000	.08066	-.08061
.14000	.08420	-.08420
.16000	.08722	-.08729
.18000	.08982	-.08997
.20000	.09205	-.09227
.22000	.09396	-.09423
.24000	.09557	-.09587
.26000	.09694	-.09722
.28000	.09803	-.09828
.30000	.09890	-.09908
.32000	.09954	-.09962
.34000	.09995	-.09986

$\frac{x}{c}$	$\frac{y}{c}$	
	UPPER SURFACE	LOWER SURFACE
.36000	.10013	-.09980
.38000	.10018	-.09946
.40000	.09999	-.09886
.42000	.09956	-.09791
.44000	.09888	-.09658
.46000	.09798	-.09496
.48000	.09682	-.09293
.50000	.09538	-.09040
.52000	.09360	-.08742
.54000	.09155	-.08404
.56000	.08926	-.08030
.58000	.08664	-.07624
.60000	.08379	-.07187
.62000	.08072	-.06728
.64000	.07754	-.06258
.66000	.07414	-.05774
.68000	.07055	-.05279
.70000	.06674	-.04770
.72000	.06284	-.04260
.74000	.05875	-.03747

(Cont'd)

TABLE II.- AIRFOIL 4-20 SECTION COORDINATES

$\frac{x}{c}$	$\frac{y}{c}$	
	UPPER SURFACE	LOWER SURFACE
.76000	.05456	-.03232
.78000	.05022	-.02734
.80000	.04579	-.02243
.82000	.04130	-.01770
.84000	.03668	-.01332
.86000	.03203	-.00931
.88000	.02739	-.00595
.90000	.02279	-.00343
.92000	.01826	-.00186
.94000	.01372	-.00140
.96000	.00909	-.00213
.98000	.00449	-.00417
1.00000	-.00005	-.00771

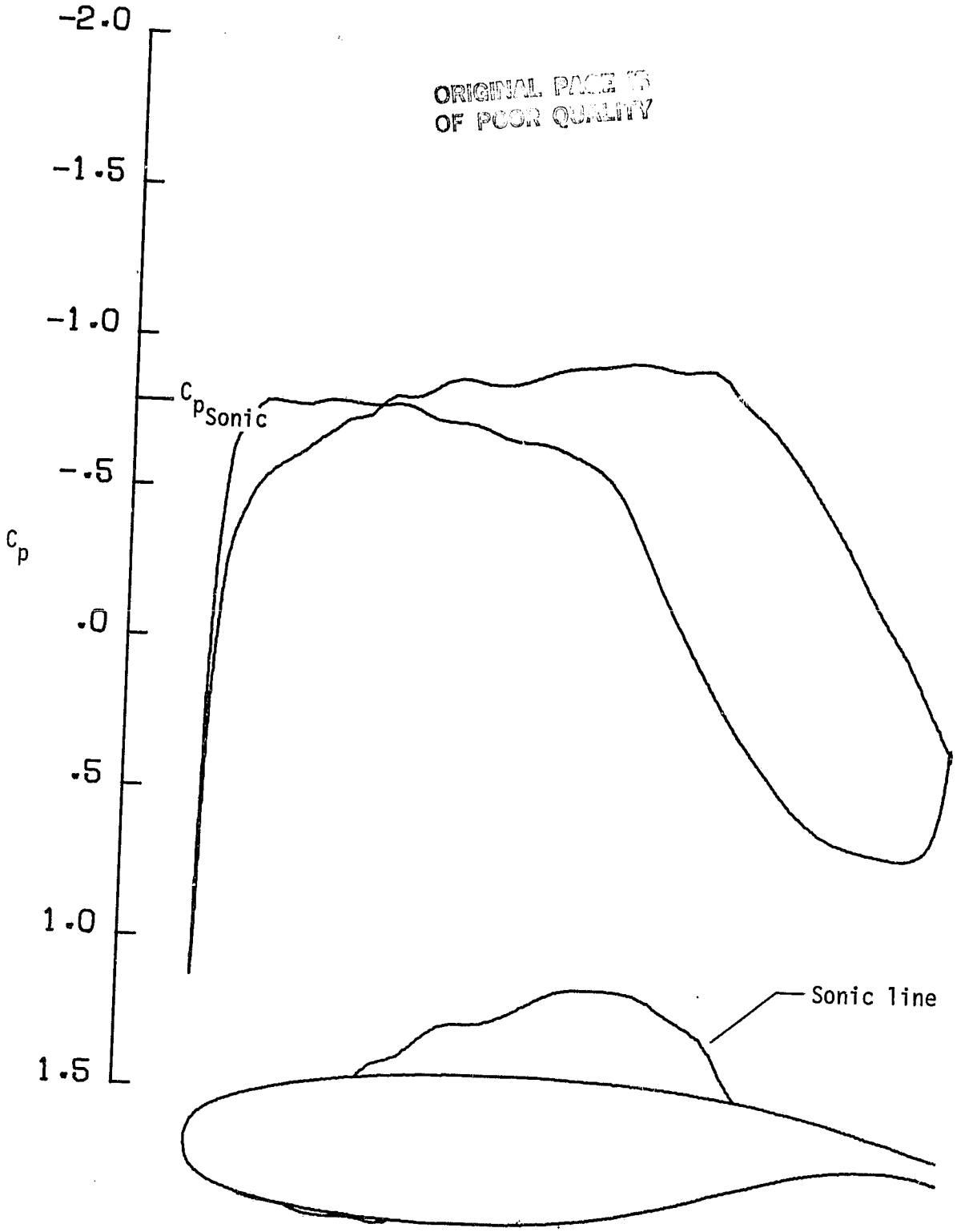

Figure 1.- Pressure distribution at $C_l = 0.40$ and $M = 0.70$ for 20-percent-thick airfoil obtained by scaling the vertical coordinates of an originally 14-percent-thick supercritical airfoil having a design $C_l \approx 0.7$.

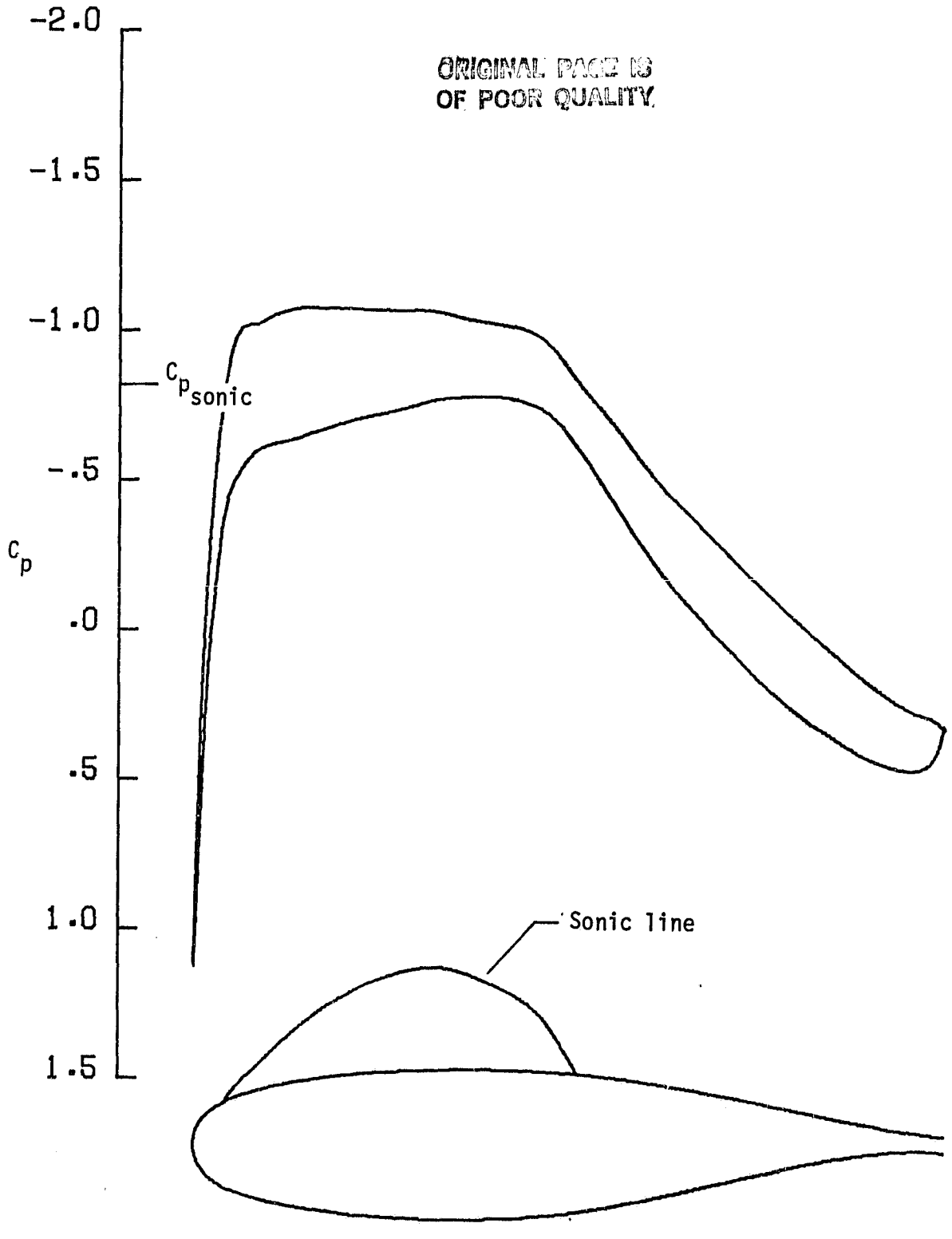

(a) M = 0.69.

Figure 2.- Pressure distribution of airfoil 3-20 at design lift coefficient.

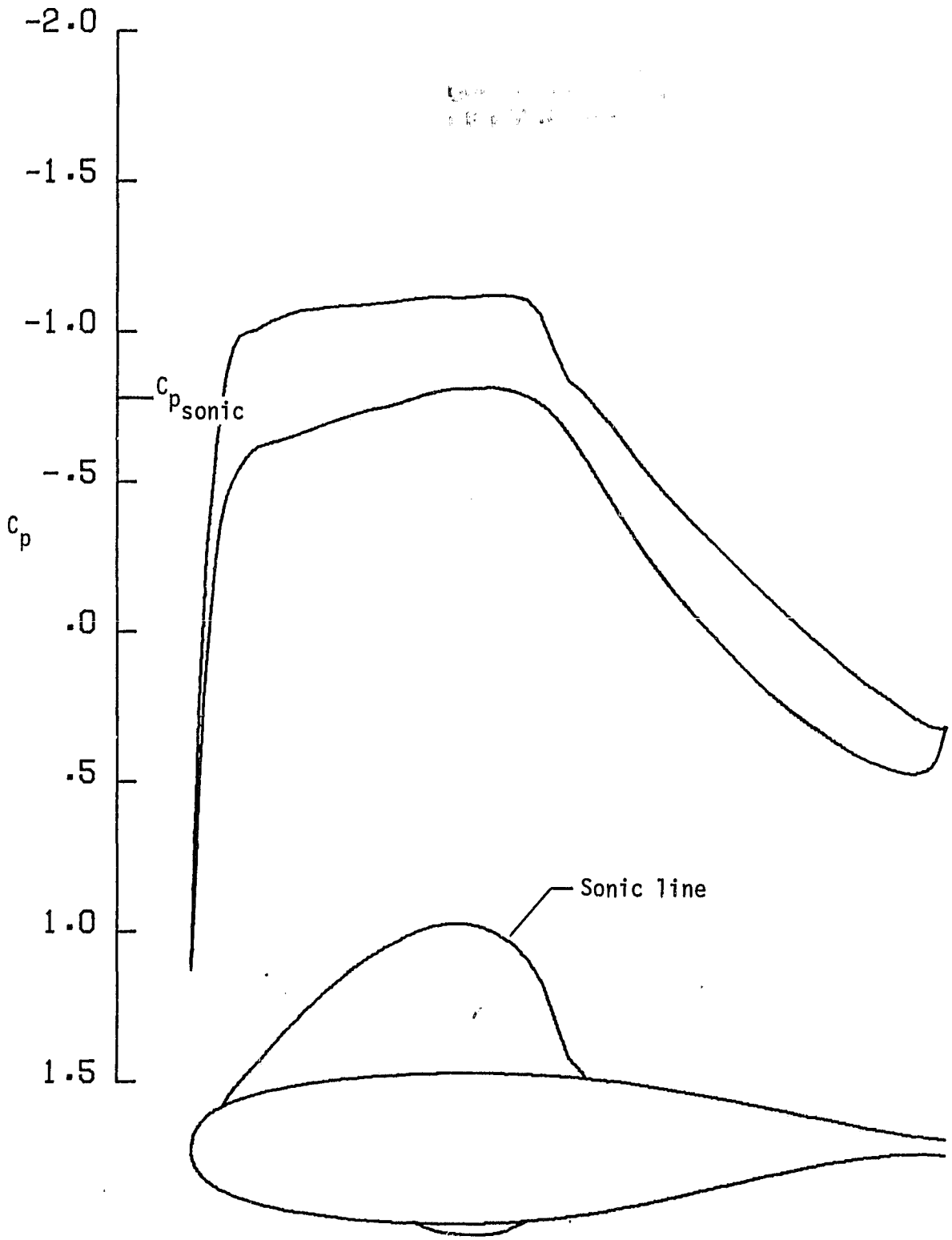

(b) M = 0.70.

Figure 2.- Continued.

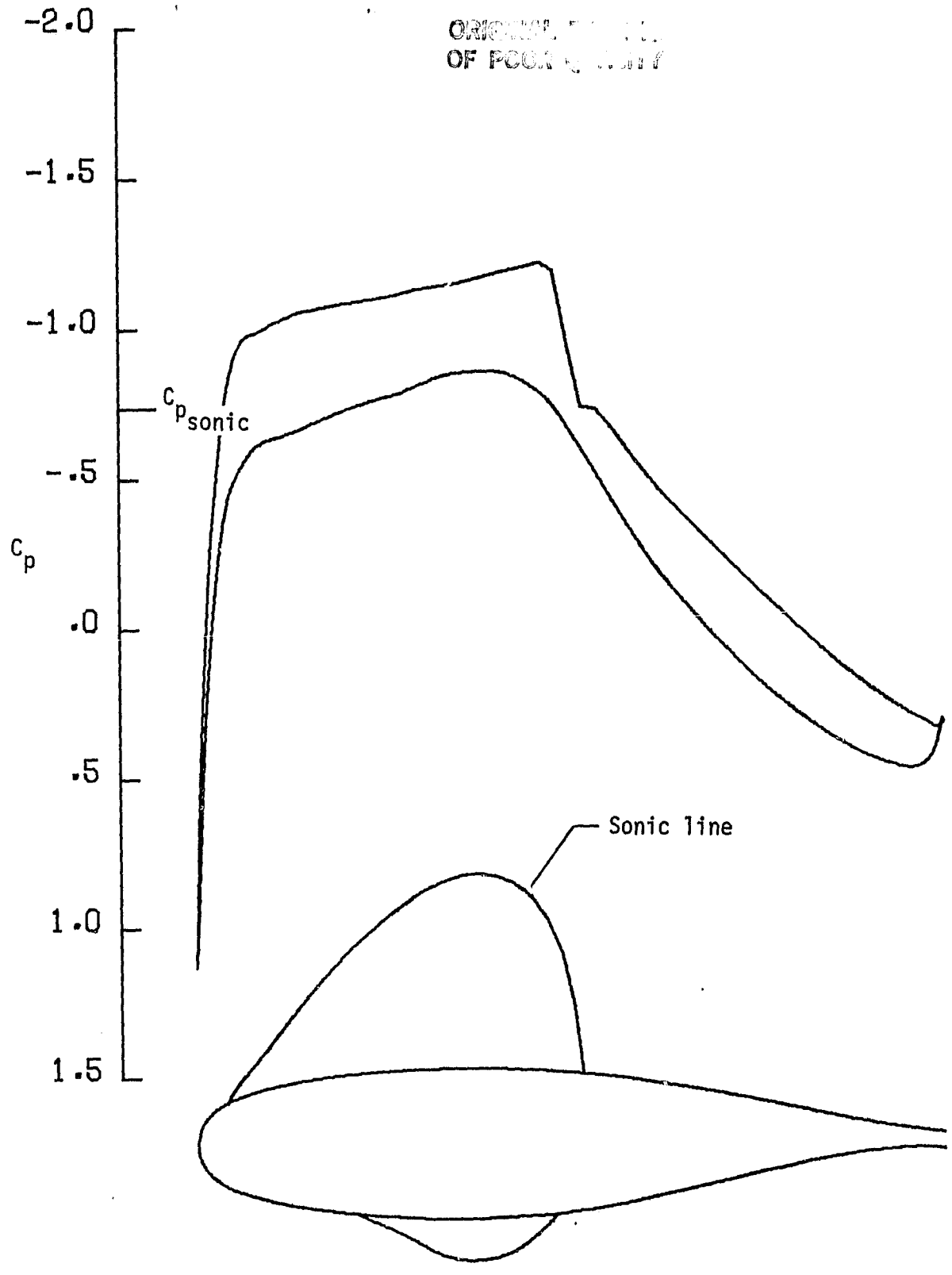

(c) M = 0.71.

Figure 2.- Continued.

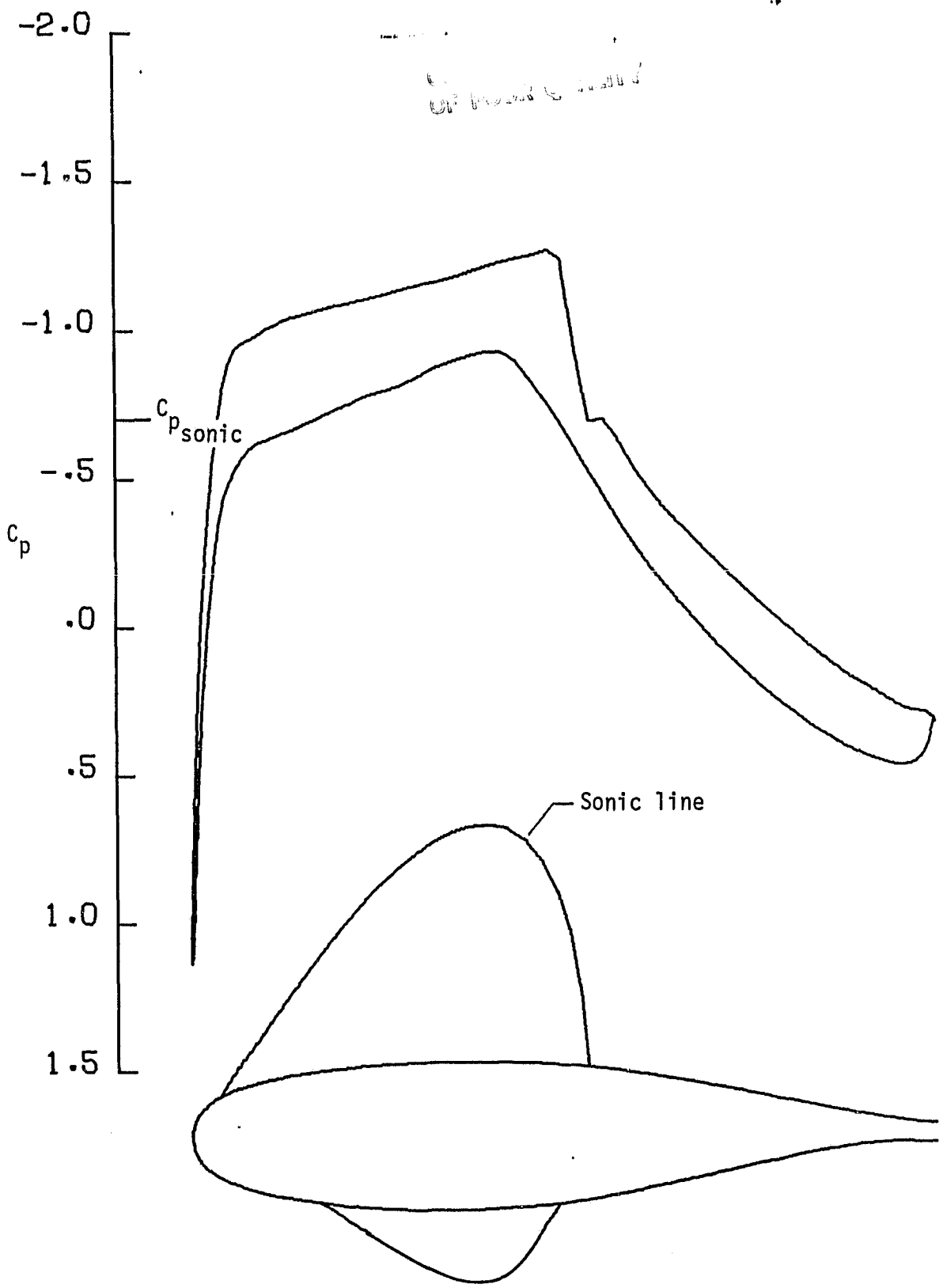

(d) M = 0.72.

Figure 2.- Concluded.

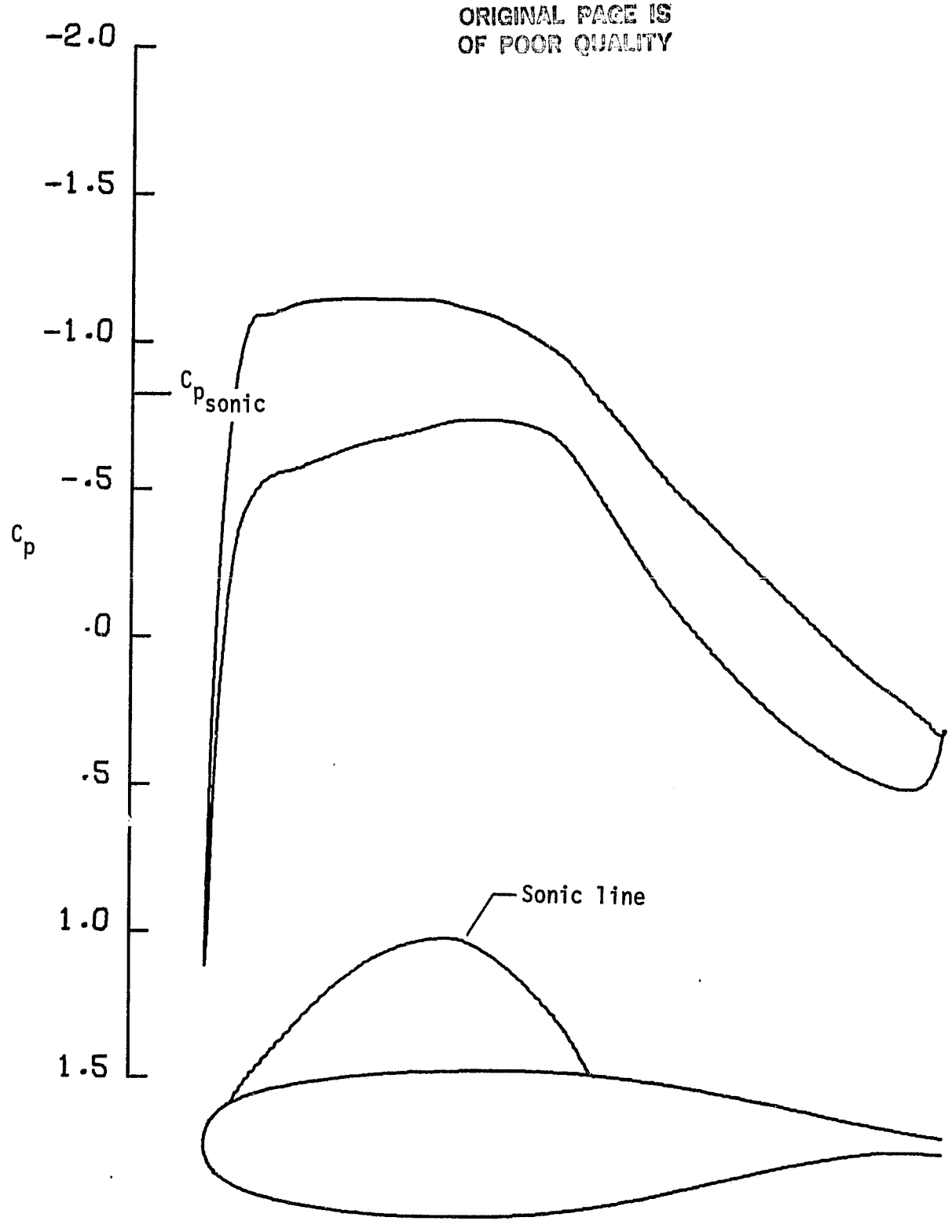

(a) M = 0.69.

Figure 3.- Pressure distribution of airfoil 4-20 at design lift coefficient.

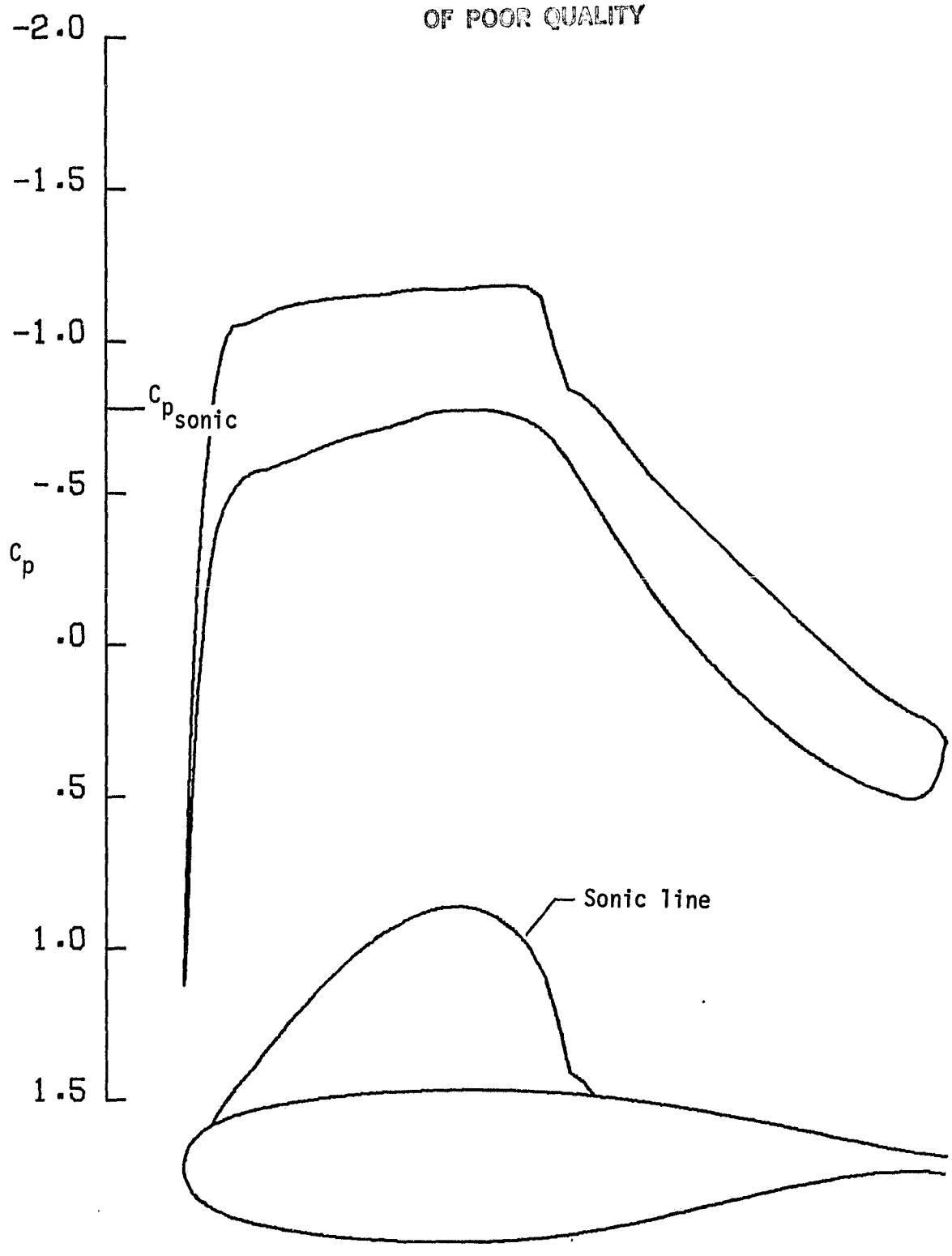

(b) M = 0.70.

Figure 3.- Continued.

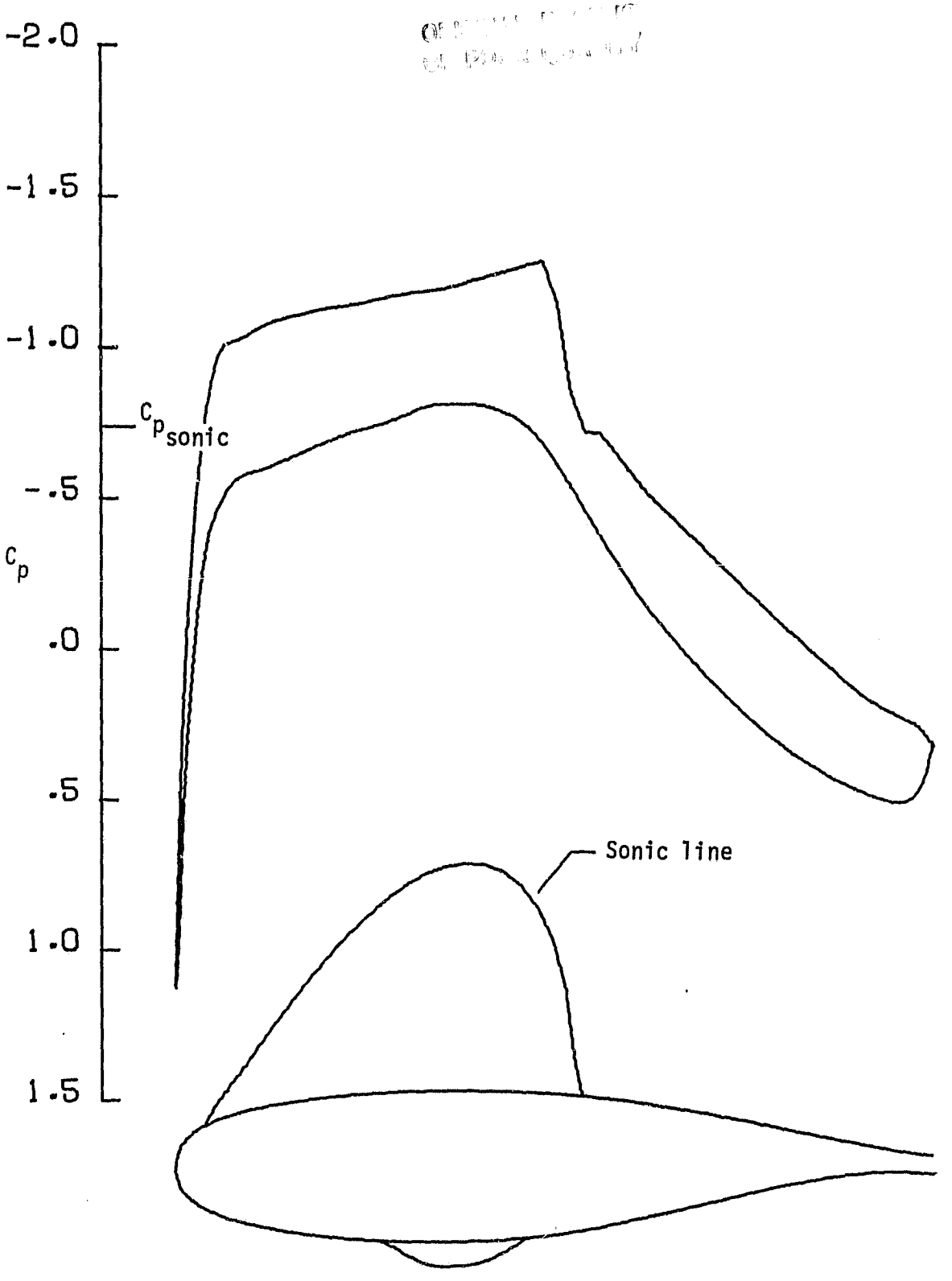

(c) M = 0.71.

Figure 3.- Concluded.

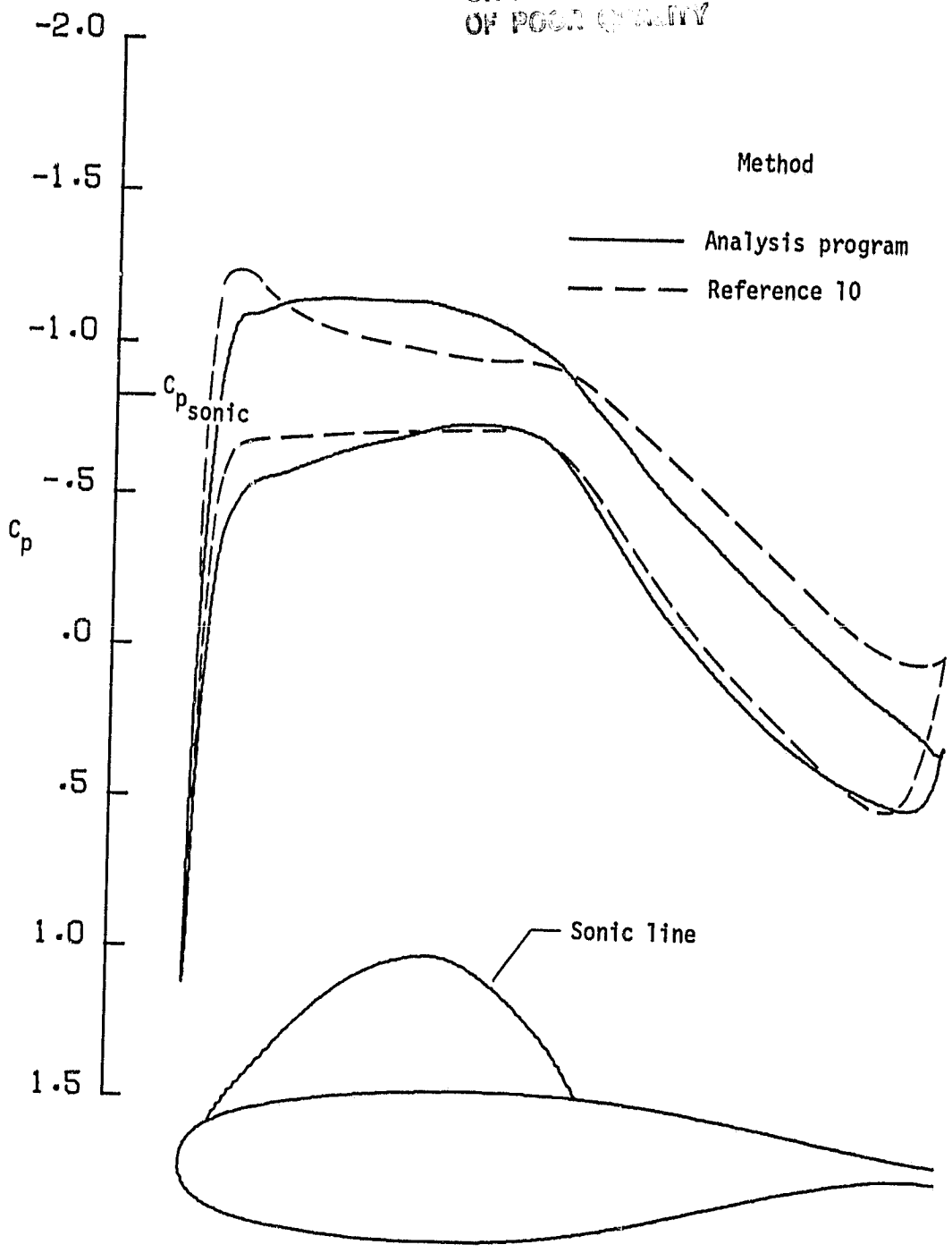

(a) M = 0.69.

Figure 4.- Comparison of pressure distributions obtained by analysis program and method of reference 10; airfoil 4-20 at design lift coefficient. Transition specified at 8- percent chord station in both calculations.

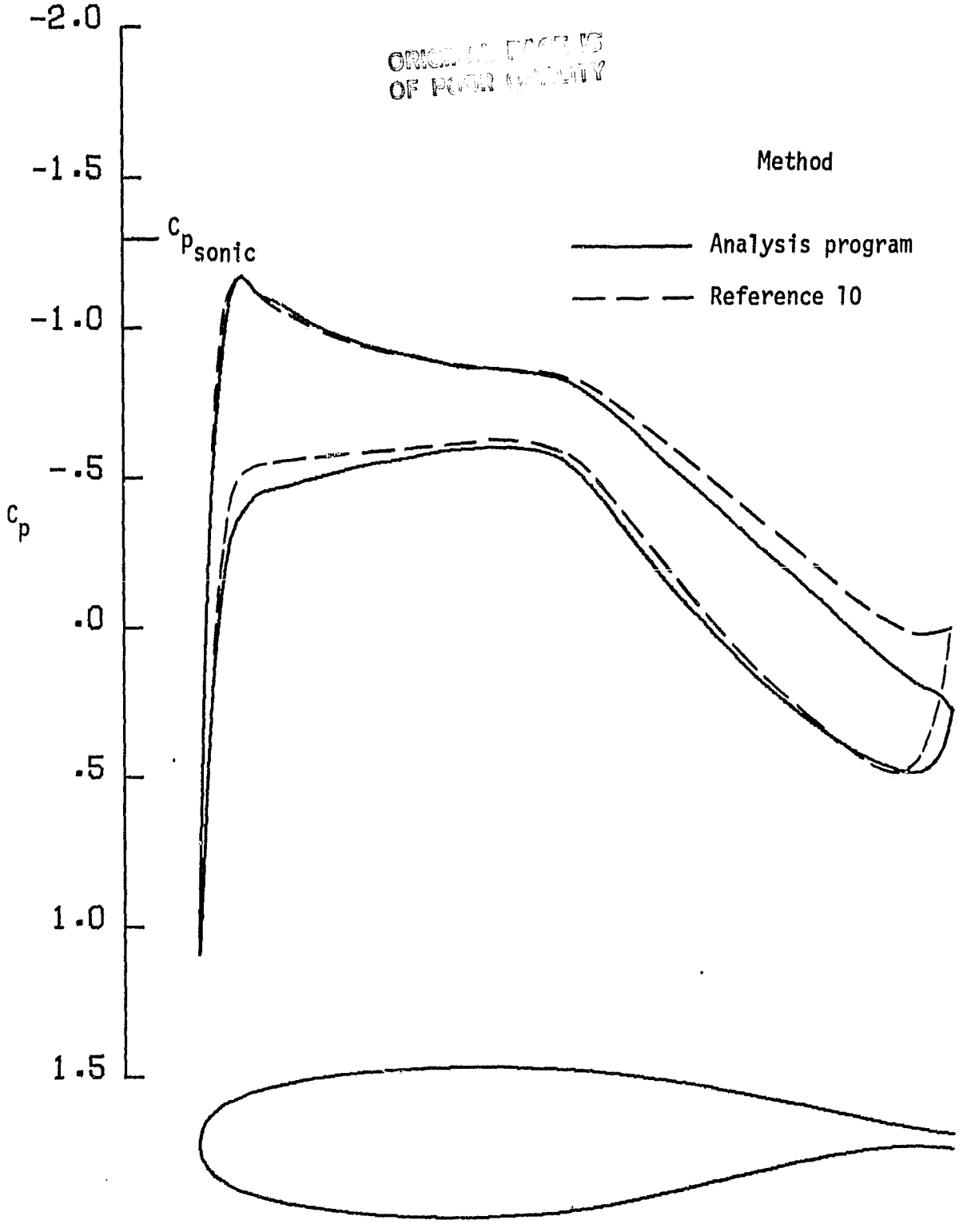

(b) M = 0.60.

Figure 4.- Concluded.

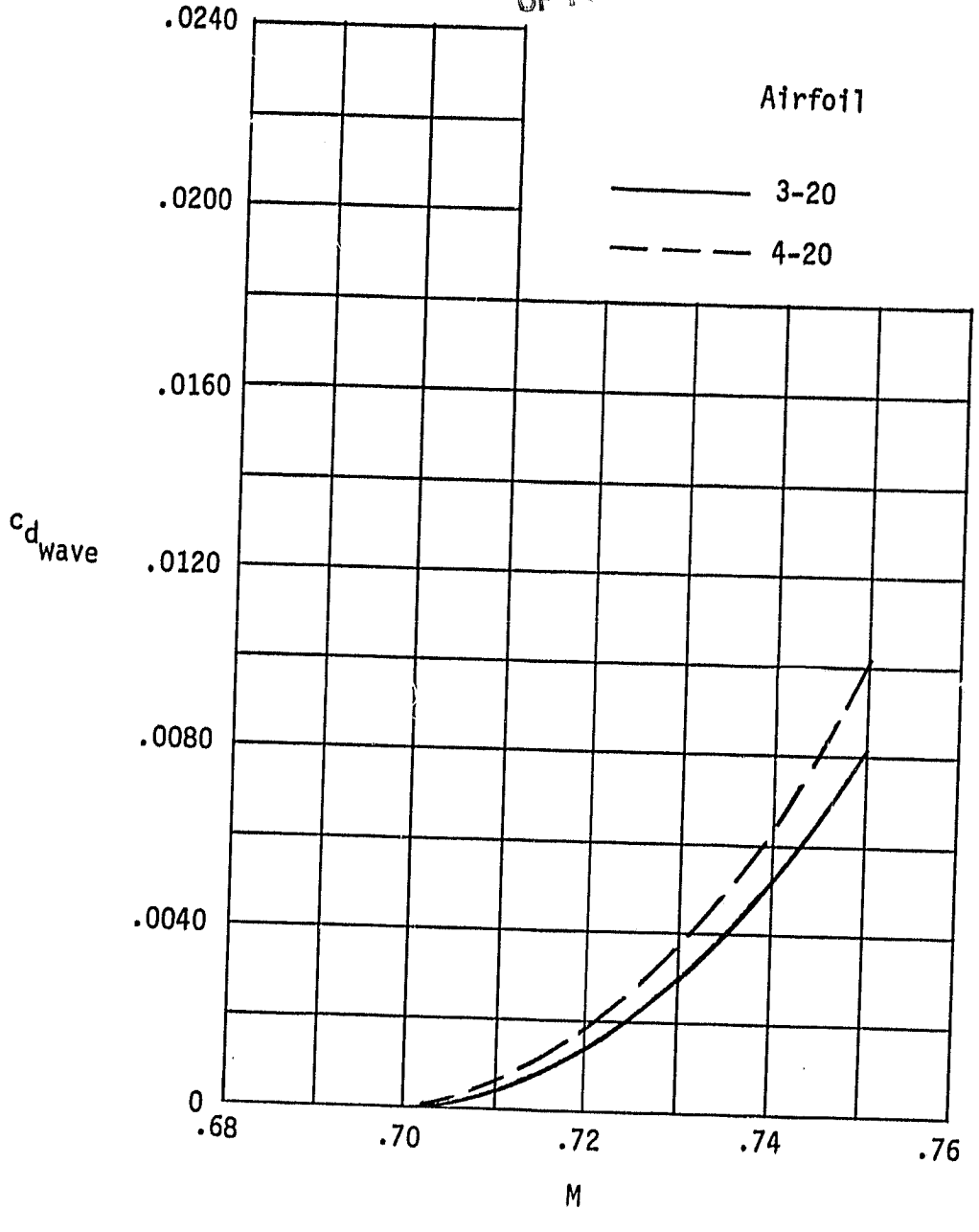

Figure 5.- Effect of Mach number on wave drag coefficient at design lift coefficient.

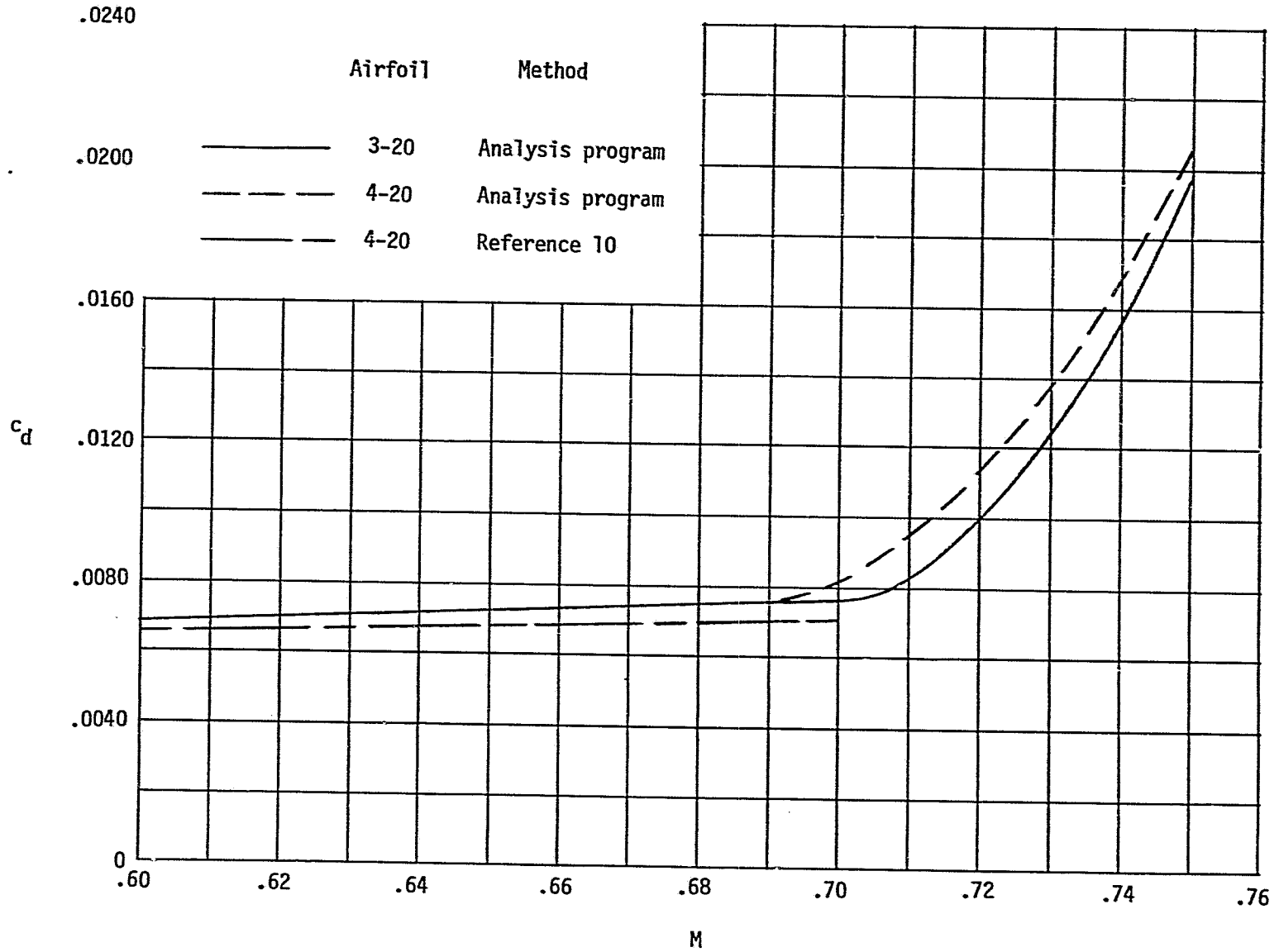

Figure 6.- Effects of Mach number on total drag coefficient at design lift coefficient as predicted by analysis program and method of reference 10.

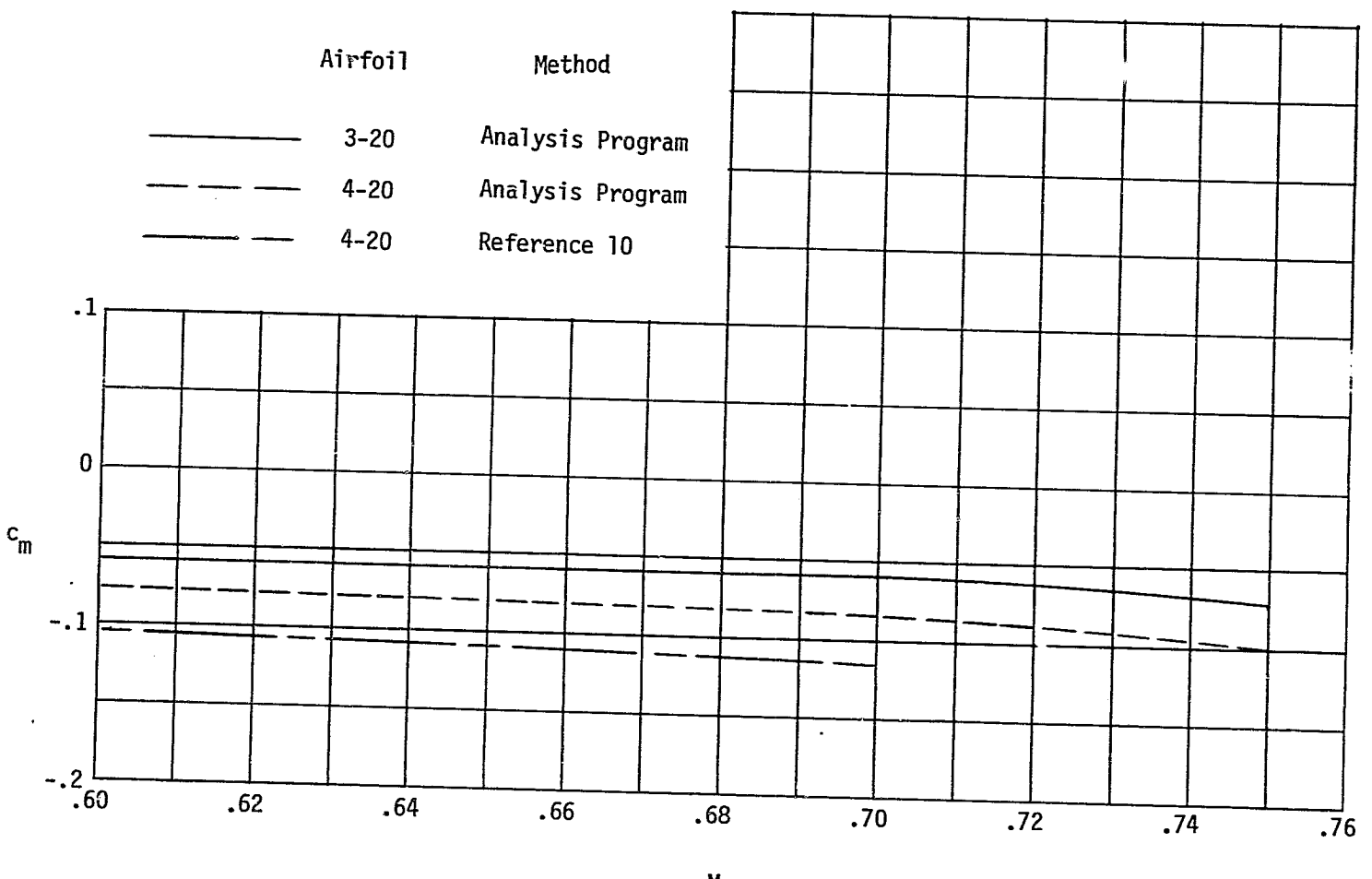

Figure 7.- Effects of Mach number on pitching-moment coefficient at design lift coefficient as predicted by analysis program and method of reference 10.

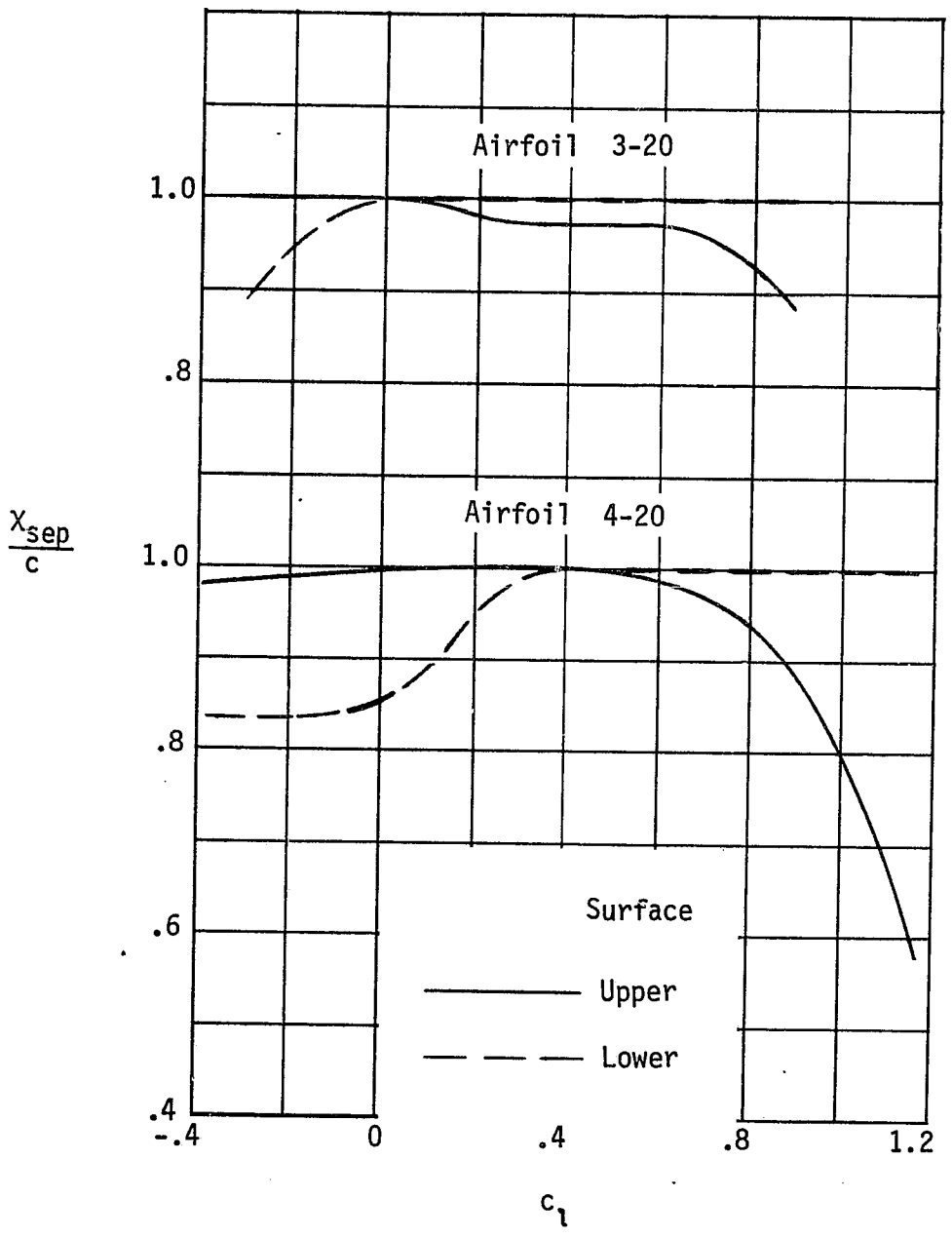

Figure 8.- Effects of lift coefficient on flow-seperation location; M = 0.69.

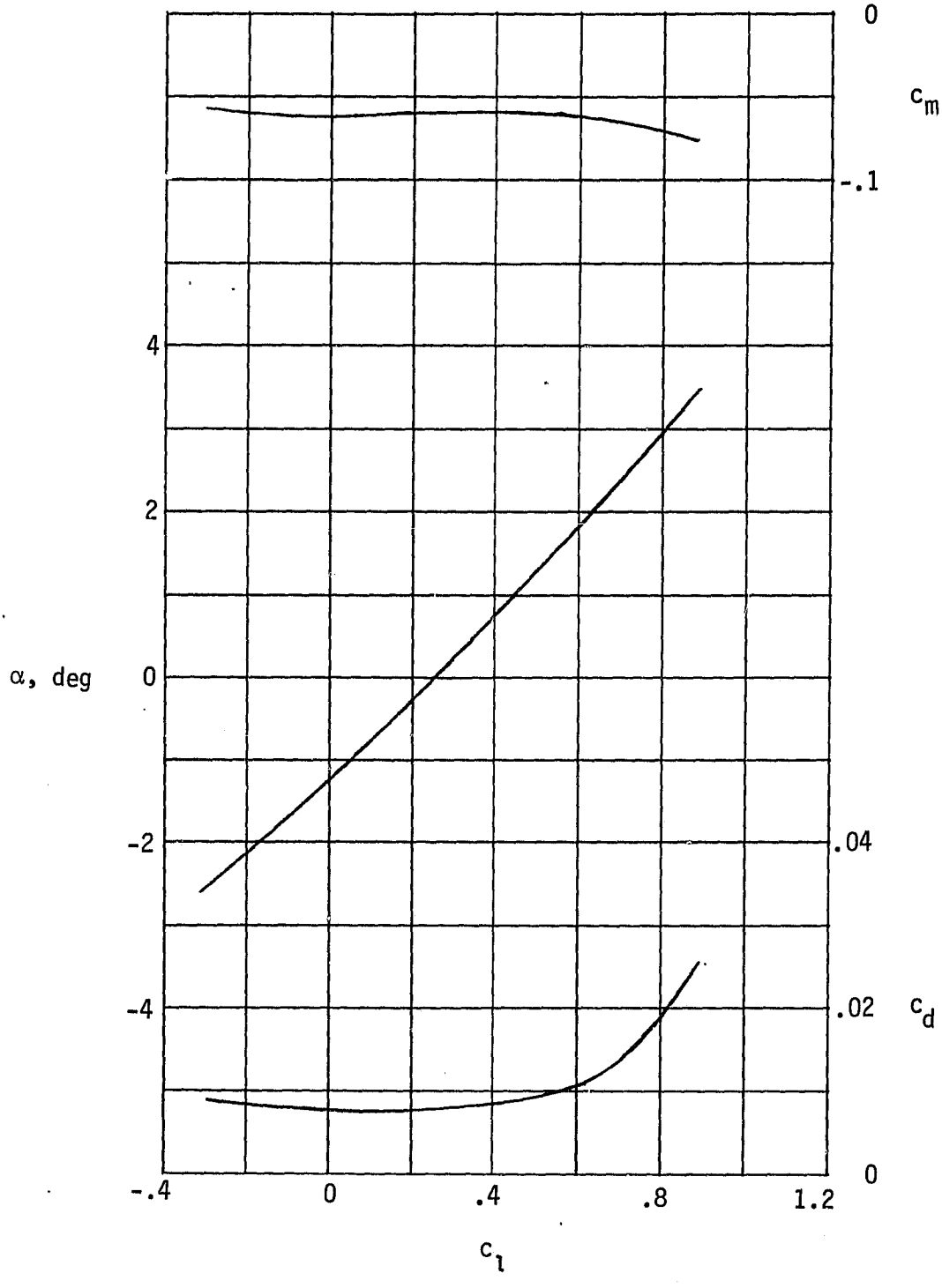

Figure 9.- Aerodynamic characteristics for airfoil 3-20; M = 0.69.

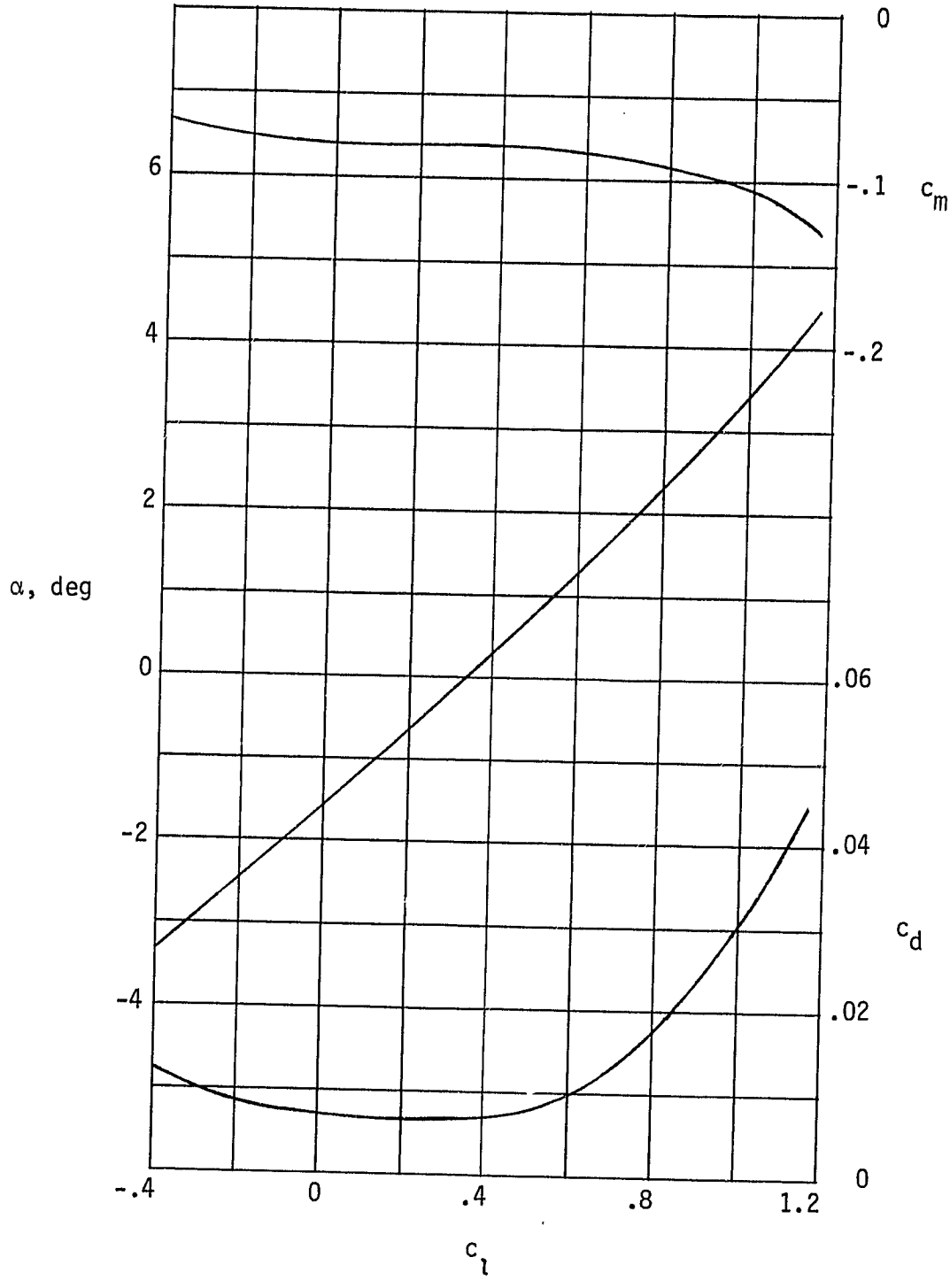

Figure 10.- Aerodynamic characteristics for airfoil 4-20; M = 0.69.